Cytoplasmic Polyamines as Permeant Blockers and Modulators of the Voltage-Gated Sodium Channel

Chien-Jung Huang* and Edward Moczydlowski*†
Departments of *Pharmacology and †Cellular and Molecular Physiology, Yale University School of Medicine, New Haven, Connecticut 06520-8066 USA

ABSTRACT We report that voltage-gated Na^+ channels (Na_V) from rat muscle (μ1) expressed in HEK293 cells exhibit anomalous rectification of whole-cell outward current under conditions of symmetrical Na^+. This behavior gradually fades with time after membrane break-in, as if a diffusible blocking substance in the cytoplasm is slowly diluted by the pipette solution. The degree of such block and rectification is markedly altered by various mutations of the conserved Lys(III) residue in Domain III of the Na_V channel selectivity filter (DEKA locus), a principal determinant of inorganic ion selectivity and organic cation permeation. Using whole-cell and macropatch recording techniques, we show that two ubiquitous polyamines, spermine and spermidine, are potent voltage-dependent cytoplasmic blockers of μ1 Na_V current that exhibit relief of block at high positive voltage, a phenomenon that is also enhanced by certain mutations of the Lys(III) residue. In addition, we find that polyamines alter the apparent rate of macroscopic inactivation and exhibit a use-dependent blocking phenomenon reminiscent of the action of local anesthetics. In the presence of a physiological Na^+/K^+ gradient, spermine also inhibits inward Na_V current and shifts the voltage dependence of activation and inactivation. Similarities between the endogenous blocking phenomenon observed in whole cells and polyamine block characterized in excised patches suggest that polyamines or related metabolites may function as endogenous modulators of Na_V channel activity.

INTRODUCTION

Voltage-gated Na^+ channels (Na_V channels) perform a critical role in electrical signaling processes of excitable cells by mediating the rapid depolarizing phase of action potentials in skeletal muscle, heart and neurons. Na_V channels are also the pharmacological target of a class of clinically important drugs that includes local anesthetics (LAs), antiarrhythmics, and anticonvulsants (Catterall, 2000; Taylor and Narasimhan, 1997). Ionic selectivity for inorganic cations and the relative permeability of various organic cations are controlled by a narrow region of the Na_V channel pore called the selectivity filter (Armstrong and Hille, 1998). In Na_V channels and homologous voltage-gated Ca^{2+} channels (Ca_V), the selectivity filter appears to be intimately related to a ring-like set of mostly charged residues called the DEKA locus and EEEE locus, respectively (Heinemann et al., 1992; Yang et al., 1993). In particular, a conserved Lys residue in the Domain III position of the DEKA locus, Lys(III), is a major determinant of organic cation permeability or molecular sieving behavior of the Na_V channel (Sun et al., 1997). Recently, we found that certain mutations of the Lys(III) residue of the rat muscle Na_V channel apparently enhance outward permeation of large symmetrical tetra-alkylammonium (TAA^+) cations, such as tetrapentylammonium, as monitored by a phenomenon called voltage-dependent relief of block (Huang et al., 2000).

Linear aliphatic polyamines (PAs) such as spermidine and spermine are ubiquitous cytoplasmic metabolites, organic cations that play a role in cell growth, differentiation, and protein synthesis (Igarashi and Kashiwagi, 2000). PAs have also been found to function as endogenous blockers and/or activators of several major classes of cation channels, such as inward rectifier K^+ channels (K_{IR}) (Nichols and Lopatin, 1997), cyclic nucleotide-gated (CNG) channels (Lu and Ding, 1999), glutamate-activated receptor (GluR) channels (Williams, 1997), nicotinic acetylcholine receptor (nAchR) channels (Haghighi and Cooper, 1998, 2000), and Ca_V channels (Scott et al., 1993). As one specific example of their importance in regulating excitability, intracellular PAs are largely responsible for strong inward rectification of certain isoforms of K_{IR} channels (Nichols et al., 1996). PAs produce such rectification by virtue of their ability to block K_{IR} channels from the cytoplasmic side in a steeply voltage-dependent fashion (Lopatin et al., 1995). Despite increasing recognition of PAs as important modulators of numerous types of channel-mediated current, the effect of PAs on Na_V channels has previously received little attention.

In this paper, we describe an anomalous time-dependent rectification phenomenon exhibited by the μ1 rat muscle Na_V channel expressed in human HEK293 cells when recorded under conditions of symmetrical Na^+ in the whole-cell configuration. To investigate the role of PAs in this cellular phenomenon, we studied the effect of cytoplasmic spermine and spermidine on Na_V channel current in a series of whole-cell and excised patch experiments. These latter PAs reversibly block the μ1 Na_V channel in a voltage-dependent fashion. Relief of PA block observed at high

Received for publication 26 September 2000 and in final form 27 December 2000.

Address reprint requests to Dr. Edward Moczydlowski, Department of Pharmacology, Yale University School of Medicine, P.O. Box 208066, 333 Cedar Street, New Haven, CT 06520-8066. Tel: 203-436-3990; Fax: 203-436-4886; E-mail: edward.moczydlowski@yale.edu.

0006-3495/01/03/1262/18 $2.00

positive voltage implies that such PAs can also permeate through the wild-type Na_V channel. The effect of certain mutations of the Lys(III) selectivity filter residue in facilitating relief of block indicates that this residue is an important determinant of PA permeability. Marked similarities between the endogenous rectification behavior observed in whole cells and PA block in macropatches suggest that PAs or a related molecule may mediate the endogenous blocking phenomenon. The effects of intracellular spermine on Na_V channel activity in the presence of a physiological Na^+/K^+ gradient are quite complex and appear to involve both block of ion conduction and shifts of voltage-dependent gating. Spermine and spermidine were found to affect the apparent rate of macroscopic inactivation and also exhibit a use-dependent blocking phenomenon. The latter effect is analogous to that of LA drugs and implies that binding site(s) for PAs and LAs overlap or allosterically interact. This raises the possibility that PAs may engage in molecular interactions with LAs and affect pharmacological properties of drugs that act on Na_V channels.

MATERIALS AND METHODS

Channel expression and cell culture

Wild-type and mutants of the μ1 rat skeletal muscle Na_V channel isoform (Trimmer et al., 1989) were constructed, subcloned into pcDNA3 expression vector, and stably expressed in HEK293 cells as previously described (Favre et al., 1996; Sun et al., 1997; Huang et al., 2000). Wild-type, K1237R, K1237H, and K1237A mutant Na_V channels are denoted, respectively, as DEKA, DERA, DEHA, and DEAA indicating the single letter code for selectivity filter residues in homologous Domains I-IV. HEK293 cells were grown at 37°C using Dulbecco's modified essential medium (Gibco BRL, Grand Island, NY) supplemented with 10% fetal bovine serum plus 500 μg/ml G-418 (Geneticin, Gibco BRL) and subdivided every 3 to 4 days. For electrophysiological experiments, cells were grown on small polylysine-coated coverslips and used for recording after 2 to 3 days in culture.

Solutions and electrophysiology

For whole-cell recording, standard 140 Na^+ bath (extracellular) solution was 140 mM NaCl, 3 mM KCl, 2 mM $MgCl_2$, 2 mM $CaCl_2$, 10 mM glucose, 10 mM Hepes-NaOH, pH 7.3. The whole-cell 125 Cs^+/20 Na^+ pipette (intracellular) solution was 125 mM CsF, 2 mM $MgCl_2$, 1.1 mM EGTA, 10 mM glucose, 20 mM Na-Hepes, pH 7.3 with HCl. The whole-cell 140 Na^+ pipette (intracellular) solution was 120 mM NaF, 20 mM NaH_2PO_4, 5 mM EGTA, 10 mM glucose, pH 7.3 with NaOH.

For inside-out macropatch recording, the standard pipette (extracellular) solution was the same Na^+ bath solution as described above for whole-cell recording. The macropatch 140 Na^+ bath (intracellular) solution was 120 mM NaF, 10 NaCl, 10 mM NaH_2PO_4, 1.5 mM EGTA, 10 mM glucose, pH 7.3 with NaOH. The macropatch 120 Cs^+/20 Na^+ bath (intracellular side) solution was 120 mM CsF, 10 NaCl, 10 mM NaH_2PO_4, 1.5 mM EGTA, 10 mM glucose, pH 7.3 with CsOH. The macropatch 135 K^+ bath (intracellular side) solution was 120 mM KF, 5 KCl, 10 KH_2PO_4, 3 NaCl, 1 mM $MgCl_2$, 1.5 mM EGTA, 10 mM glucose, pH 7.3 with KOH. Solutions containing spermine or spermidine (Sigma, St. Louis, MO) were prepared by addition of these polyamines to the above internal solutions at the desired final concentration.

Electrophysiological recording was performed at room temperature (23°C) using an HEKA EPC-9 amplifier with Pulse and Pulse-fit software (Instrutech, Great Neck, NY). The resistance of whole-cell patch pipettes fabricated from Kimax-51 glass capillaries (Fisher Scientific, Pittsburgh, PA) was 1 to 2 MΩ when filled with Cs^+/Na^+ or Na^+ pipette solution. The resistance of macropatch pipettes was 0.5 to 0.7 MΩ when filled with extracellular Na^+ solution. Current records were digitally acquired by filtering at 10 kHz and sampling at 50 kHz. Data traces were subsequently filtered at 3 KHz for analysis and presentation. For both whole-cell and macropatch recordings, capacitance transients and leak currents were subtracted by using a positive P/5 pulse protocol delivered at -140 mV. For whole-cell recording, series resistance was electronically compensated to at least 70%. A KCl-agar bridge was used to connect the bath solution to the Ag/AgCl ground electrode.

Current-voltage behavior of Na_V channels was typically monitored by recording the response to a consecutive series of step voltage pulses 10 ms in duration to membrane potentials ranging between -140 and $+200$ mV at 10-mV increments. The holding potential and pulse interval were normally -120 mV and 0.5 s, respectively. Whole-cell data was usually collected beginning at 10 min from the time of break-in, except for experiments for investigating time dependence of I-V behavior (e.g., Fig. 2). Recording from excised macropatches was initiated after outward currents exhibited a stable response during continuous gravity perfusion of control bath solution.

Tonic block by PAs was monitored with 10-ms test pulses to $+100$ mV from a holding potential of -120 mV, delivered at 10- or 20-s intervals. The time dependence of use-dependent or phasic block by PAs was monitored for 50 s by stimulating with a consecutive train of 3.25-ms test pulses to $+50$, $+100$, $+150$, or $+200$ mV delivered at a frequency of 4 Hz from a holding potential of -120 mV. In the absence of PAs, the decline of control peak currents due to cumulative inactivation during 4 Hz stimulation was usually $<10\%$ after 50 s; otherwise, the patch was discarded from the data set. Steady-state availability due to fast inactivation was measured from the response of a 10-ms test pulse to -20 mV following conditioning prepulses of 250 ms over a series of voltages ranging from -140 to $+40$ mV in 10-mV increments.

Data analysis and modeling

This study focuses on the behavior of peak macroscopic currents generated by Na_V channels that display normal rapid inactivation. Average behavior was determined as the mean ($\pm$ SE) from data samples of 3–10 cells or macropatches for each set of experimental conditions. Except for Fig. 2, *A* and *B*, which illustrates results from a typical cell, most experimental results are plotted as average normalized peak I-V relations. For purpose of presentation, peak I-V data collected from a given cell were normalized in two different ways. For the first method, denoted on ordinate axes by I(Norm), each peak current value collected from a given cell/patch was divided by the absolute value of the maximum inward peak current (usually evoked at -20 mV) from the same cell/patch (e.g., Fig. 1 *A*, Fig. 4, *B* and *C*, and Fig. 10 *B*). For the second normalization method, denoted on ordinate axes by $I(Norm)_{100}$, each peak current value collected from a given cell/patch was divided by the actual or expected peak current value in the absence of PA at $+100$ mV (e.g., Fig. 1 *B*, Fig. 2, *A* and *B*, Fig. 3, *A–D*, Fig. 6, *B* and *C*, and Fig. 7, *B* and *C*).

Normalized membrane conductance versus voltage, plotted in Figs. 6 and 7, was fit with a simple model of a permeant blocker described elsewhere in more detail (Huang et al., 2000). The model is represented by the following scheme:

$$B_{in} + O \underset{k_{-1}}{\overset{k_1[B]}{\rightleftharpoons}} O{\cdot}B \xrightarrow{k_{-2}} O + B_{out}$$

where an internal blocker, B_{in}, binds to an internally accessible site in the open channel, *O*, with an equilibrium dissociation constant, $K_1 = k_{-1}/k_1$.

Binding of B_{in} results in a blocked state, $O \cdot B$. Unblocking of the channel can either occur by dissociation of the blocker back to the inside governed by the k_{-1} rate constant, or by outward permeation of the blocker governed by the k_{-2} rate constant. For an ohmic channel, the relative conductance in the presence of blocker to that in the absence of blocker is given by:

$$G/G_{max} = \{1 + [B]_{in}/K_B(V)\}^{-1} \quad (1)$$

where G_{max} is the maximal unblocked conductance, $[B]_{in}$ is the internal blocker concentration, and $K_B(V)$ is an apparent voltage-dependent blocker dissociation constant. G_{max} is determined by the conductance measured from the peak current versus voltage relation from the same cell/patch before application of PA blocker. $K_B(V)$ may be represented as

$$K_B(V) = K_1(V)/[1 + K_R(V)] \quad (2)$$

$$K_1(V) = K_1(0)\exp(-z'_1V/A) \quad (3)$$

$$K_R(V) = K_R(0)\exp(z'_2V/A) \quad (4)$$

In Eq. 2, $K_1(V) = k_{-1}(V)/k_1(V)$ and $K_R(V) = k_{-2}(V)/k_{-1}(V)$. $K_1(V)$ is the voltage-dependent form of the blocker dissociation constant in the absence of outward permeation. $K_R(V)$ is the ratio of voltage-dependent rate constants for blocker dissociation to the outside of the cell over that for dissociation back to the inside of the cell. In Eqs. 3 and 4, V is membrane voltage and $A = 25.4$ mV. $K_1(0)$ and $R(0)$ are values of the respective constants at 0 mV, whereas z'_1 and z'_2 are unitless parameters that describe the relative magnitude of apparent voltage dependence.

Steady-state availability describing voltage-dependent inactivation and normalized conductance curves describing voltage-dependent activation were fit to simple transforms of a Boltzmann function given in the legend to Fig. 10. Nonlinear fitting of data to theoretical equations was performed with the Marquardt-Levenberg routine of Sigmaplot 4.0 (SPSS Inc., Chicago, IL).

RESULTS

The Lys(III) residue of the DEKA locus determines rectification of outward current

Our interest in the interaction of PAs with Na_V channels arose from observations on the role of the DEKA locus or selectivity filter in controlling rectification of outward current. The experiment of Fig. 1 *A* compares the macroscopic current-voltage behavior of wild-type (DEKA) and mutant (DEAA) μ1 Na_V channels using whole-cell recording of stably transfected HEK293 cells with 140 mM NaCl plus 3 mM KCl in the extracellular bath solution and 125 mM CsF plus 20 mM Na-Hepes in the intracellular pipette solution. Under these ionic conditions, the peak current of the wild-type channel exhibits strong inward rectification as indicated by the decrease in slope conductance as a function of positive voltage, measured here for consecutive steps of voltage from −140 to +200 mV. In contrast, the DEAA mutant exhibits much larger outward currents and a more linear peak I-V relationship at positive voltages when recorded under the same conditions (Fig. 1 *A*). The behavior of the wild-type and DEAA mutant Na_V channels can be explained by their different ionic selectivity for the alkali cations, Na^+, K^+, and Cs^+, and the transmembrane gradients of these cations. In previous work, the relative permeability of the wild-type channel for extracellular Cs^+ compared to Na^+ was found to be immeasurably small (<0.01), whereas that for the DEAA channel was $P_{Cs}/P_{Na} = 0.57$ (Sun et al., 1997). Thus, rectification of outward current through the Na^+-selective wild-type channel under the conditions of Fig. 1 *A* is due to the asymmetric Na^+ gradient (140 mM Na^+ out/20 mM Na^+ in) and the low permeability of intracellular Cs^+. (A similar example of such rectification involving block of outward Na^+ current by internal K^+, another weakly permeable alkali cation, was previously described by Garber (1988) at the single-channel level for rat muscle Na_V channels modified by batrachotoxin or veratridine.) In contrast to rectification of the wild-type channel, the practically ohmic behavior of outward current of the DEAA mutant in Fig. 1 *A* reflects its high conductance to intracellular Cs^+. This comparison shows that the Lys(III) residue of the DEKA locus controls the relative permeability of intracellular alkali cations in a manner similar to that previously described for extracellular cations (Heinemann et al., 1992; Favre et al., 1996; Sun et al. 1997).

To verify that outward current carried by Na^+ alone through the wild-type channel does not intrinsically rectify at high voltage, we performed inside-out macropatch recording using large patches excised from stably transfected HEK293 cells in the presence of symmetrical 140 mM Na^+. Results in Fig. 1 *B* show that outward peak current of the wild-type DEKA channel in the excised patch is an approximately linear function of positive voltage under conditions of symmetrical Na^+. Replacement of 140 mM Na^+ bath solution on the intracellular side of the patch with 120 mM Cs^+/20 mM Na^+ results in a strongly rectifying peak I-V relationship (Fig. 1 *B*) like that in Fig. 1 *A* for wild-type. The positive shift of reversal potential from a value close to 0 mV in symmetrical Na^+ to +50.4 ± 1.3 mV (±SE, $n = 7$) for a gradient of 147 mM Na^+ (out) and 20 mM Na^+ (in) is exactly predicted by the Nernst equation for Na^+. The experiments of Fig. 1 thus demonstrate that the Lys(III) residue of the Na_V channel selectivity filter (K1237) is a major determinant of current rectification caused by differential permeability to two different alkali cations, Na^+ and Cs^+.

Time-dependent, rectifying I-V behavior of the wild-type Na_V channel recorded in whole-cell mode in the presence of symmetrical Na^+

Based on results of the macropatch experiment of Fig. 1 *B*, one would predict that the I-V behavior of the wild-type Na_V channel in the whole-cell configuration would be an approximately linear function of positive voltage in the presence of symmetrical Na^+. Surprisingly however, we find that this is not the case, especially when I-V data are collected soon after establishing the whole-cell mode. Fig. 2 *A* shows a series of peak I-V curves from a typical HEK293 cell expressing μ1 Na_V channels recorded in whole-cell mode with symmetrical 140 mM Na^+. When a standard I-V

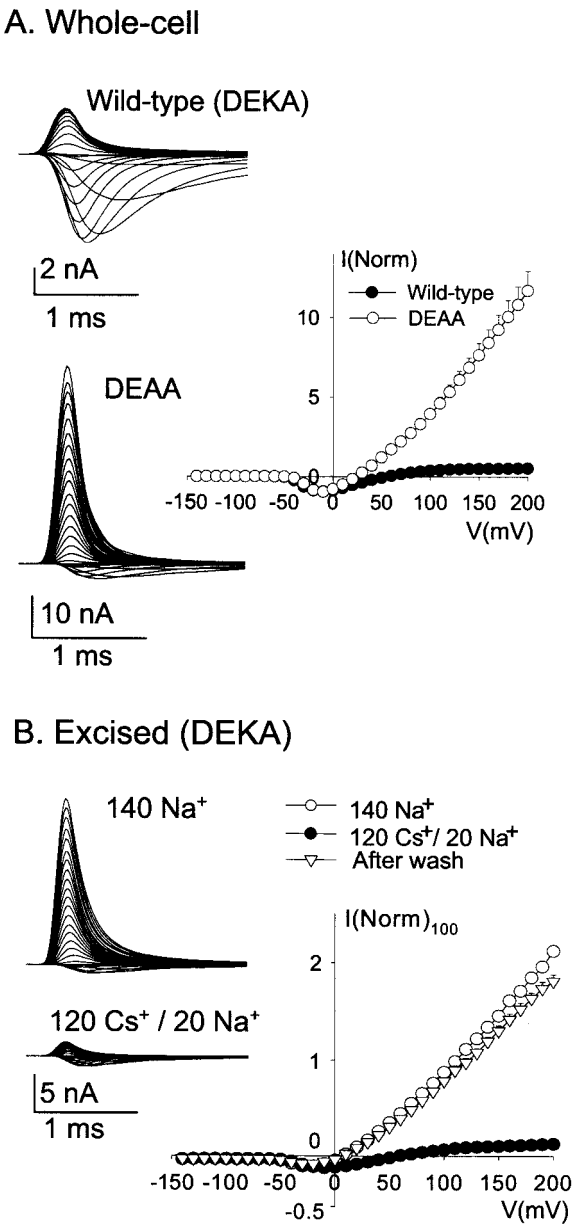

FIGURE 1 Rectification of outward current in the presence of internal Cs^+ is controlled by the K(III) residue of the DEKA locus. (*A*) Comparison of whole-cell records of wild-type (DEKA) and DEAA mutant Na_V channels in the presence of 140 mM Na^+ extracellular solution and 125 mM Cs^+/20 mM Na^+ intracellular solution. (*left*) Typical whole-cell current traces of wild-type DEKA (*top*) and DEAA (*bottom*) mutant channels, elicited with a series of 10 ms steps to voltages ranging from −140 to +200 mV in 10-mV increments from a holding potential of −120 mV. The pulse interval was 0.5 s. (*right*) Peak current-voltage relationships of wild-type and DEAA channels, normalized to the maximum peak inward current of each cell and averaged as mean ± SE of 5 to 8 cells. (*B, left)* Currents traces from an excised macropatch (inside-out) containing wild-type Na_V channels in the presence of 140 mM symmetrical Na^+ (*top*) and after replacement of the bath solution with 120 mM Cs^+/20 mM Na^+ (*bottom*). The voltage pulse protocol was the same as in (*A*). (*right*) Peak I-V data in 140 mM Na^+ control bath solution, after bath perfusion with 120 Cs^+/20 Na^+, and after return to 140 mM Na^+. Data points are normalized to control outward current at +100 mV for a given patch and averaged as mean ± SE of 7 patches.

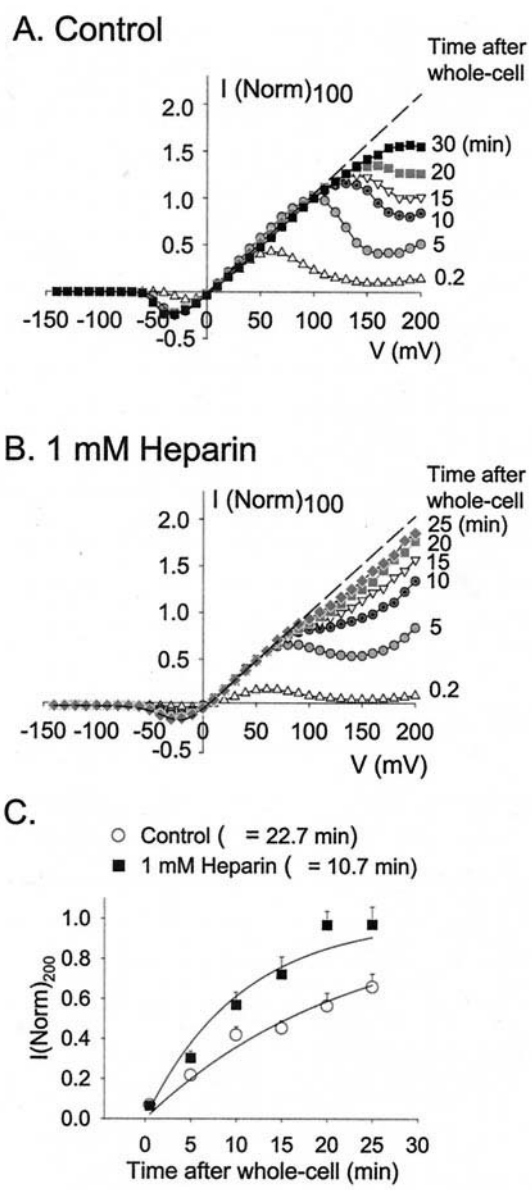

FIGURE 2 Time-dependent rectification of whole-cell I-V behavior of wild-type Na_V channels in the presence of symmetrical 140 mM Na^+. (*A*) Typical example of peak I-V relations collected from the same cell at various times ranging from 0.2 to 30 min after membrane break-in. I-V data are normalized to the expected peak current at +100 mV, assuming ohmic behavior of outward current. *Dashed line* is the expected I-V relation in the absence of intracellular block. (*B*) Effect of 1 mM internal heparin on time-dependent I-V behavior. The same experiment described in (*A*) was performed with 1 mM heparin in the pipette solution. (*C*) Average whole-cell peak currents at +200 mV as a function of time after membrane break-in, in the absence and presence of 1 mM heparin in the pipette solution. Data points are normalized to the expected peak current at +200 mV, assuming ohmic behavior of outward current and plotted as the mean ± SE of 3 to 10 cells. *Solid lines* represent the best fit to a single exponential function with time constants of 22.7 and 10.7 min in the absence and presence of heparin, respectively.

protocol (consecutive 10-ms pulses in steps of +10 mV from V_{hold} = −120 mV at intervals of 0.5 s) is recorded immediately (~0.2 min) after membrane break-in to achieve whole-cell mode, we observe an anomalous N-shaped I-V relationship characterized by a "negative resistance" region at voltages positive to +50 mV. If the same voltage-pulse protocol is used to record from the same cell at a later time, the negative-resistance region appears to gradually shift to a higher voltage range (Fig. 2 *A*). The I-V relationship becomes progressively more linear with time, such that by ~30 min after break-in, a stable and rather ohmic peak I-V relationship for outward current is finally observed. It should be noted that the I-V data in Fig. 2 were collected by using consecutive pulses of increasing voltage steps taken every 500 ms (frequency = 2 Hz), an interval that is short enough to produce use-dependent blocking behavior of Na_V channels under certain ligand conditions. Such a pulse protocol was nevertheless specifically used to quickly assay the behavior of the rapidly changing I-V relationship in whole-cell mode. Very similar results and rectification behavior were obtained by reversing the pulse sequence from the most positive to the most negative voltage step.

We hypothesize that the "negative-resistance" behavior in the positive voltage-region of Fig. 2 *A* is due to a strongly voltage-dependent block by unidentified intracellular cation(s). The intracellular pipette solution for this whole-cell experiment was specifically designed to avoid known or potential blocking cations by excluding Ca^{2+} and Mg^{2+} and by using phosphate as a pH buffer. Because the only known cations in the pipette solution are Na^+ and H^+ (pH 7.3), it seems likely that the cytoplasm of HEK293 cells must be the source of an intracellular blocking activity that dissipates with time by progressive dilution with pipette solution. If this is the case, the slow development of linear I-V behavior is surprising, given that the time constant of cell-pipette exchange of a variety of freely diffusible substances with a molecular weight (M_r) <1000 has been found to be <60 s (Pusch and Neher, 1988; Marty and Neher, 1995).

We further explored the nature of this slow diffusion phenomenon by performing similar experiments with 1 mM heparin (average M_r = 3000) added to the pipette solution. Heparin is a large sulfated polysaccharide polyanion and is expected to electrostatically adsorb organic polycations (Amann and Werle, 1956) and basic proteins. We found that this manipulation significantly increased the rate of equilibration in such whole-cell experiments, as illustrated by typical data in Fig. 2 *B*. Fig. 2 *C* shows the average time course of equilibration of outward current in such experiments as measured by the average ratio of peak current measured at +200 mV to that expected at long times by linear extrapolation from I-V data in the low positive voltage range. The limited stability of the whole-cell configuration and the slow kinetics of equilibration prevented us from collecting data at times longer than ~25 min after break-in. If we assume that this behavior follows an exponential time course, the data can be fit with an apparent time constant of 22.7 min in the absence of heparin and 10.7 min in the presence of 1 mM heparin (Fig. 2 *C*). Enhancement of the equilibration rate by heparin in the pipette solution supports the idea that the anomalous rectification phenomenon of Fig. 2 *A* is due to slow release of an endogenous cationic blocking substance present in the cytoplasm or a cellular compartment.

Anomalous rectifying whole-cell behavior depends on the residue at the K(III) position of the DEKA locus

In recording whole-cell Na_V channel currents from HEK293 cells under conditions of symmetrical 140 mM Na^+, we further observed that the exact shape of the peak I-V relation depends markedly on the particular amino acid residue substituted by mutation at the K(III) position of the DEKA locus. Fig. 3 compares average peak I-V data (n = 3 cells) for the wild-type Na_V channel and mutant substitutions of the K(III) residue by Arg (DERA), His (DEHA), and Ala (DEAA). Fig. 3 *A* shows that the average outward current of wild-type (DEKA) recorded at 5 min after membrane break-in displays a prominent negative resistance region in the positive voltage range. At 20 min after break-in, the negative resistance region is less prominent and is shifted to a higher voltage range. The behavior of DERA mutant is similar to wild-type, except that the negative resistance region is much shallower and displays a more pronounced rising phase at voltages above +120 mV (Fig. 3 *B*). In contrast, the DEHA mutant exhibits only a mild inflection in the positive voltage quadrant of the peak I-V relation (Fig. 3 *C*), and the DEAA mutant does not exhibit rectification or any obvious inflection (Fig. 3 *D*). Note also that the peak I-V data for both DEHA and DEAA displays little (Fig. 3 *C*) or no (Fig. 3 *D*) time dependence from 5 to 20 min after membrane break-in. These results imply that, whatever its origin, the mechanism of endogenous rectification must involve a molecular interaction with the K(III) residue of the Na_V channel selectivity filter.

The complex I-V behavior in Fig. 3 is readily interpreted by our hypothesis for an endogenous cationic blocking substance(s). The presence and absence of rectification in the wild-type channel versus various mutants of the K(III) residue can be explained by the fact that these mutants have altered molecular sieving behavior toward organic cations (Sun et al., 1997; Huang et al., 2000). If the postulated endogenous blocking molecule(s) are organic cations, then enhanced permeability of such molecules through the various mutant Na_V channels could account for such differences in peak I-V behavior under whole-cell conditions. We previously described such a phenomenon for the DEAA mutant, which displays enhanced permeability for large tetra-alkylammonium (TAA^+) cations such as tetrapen-

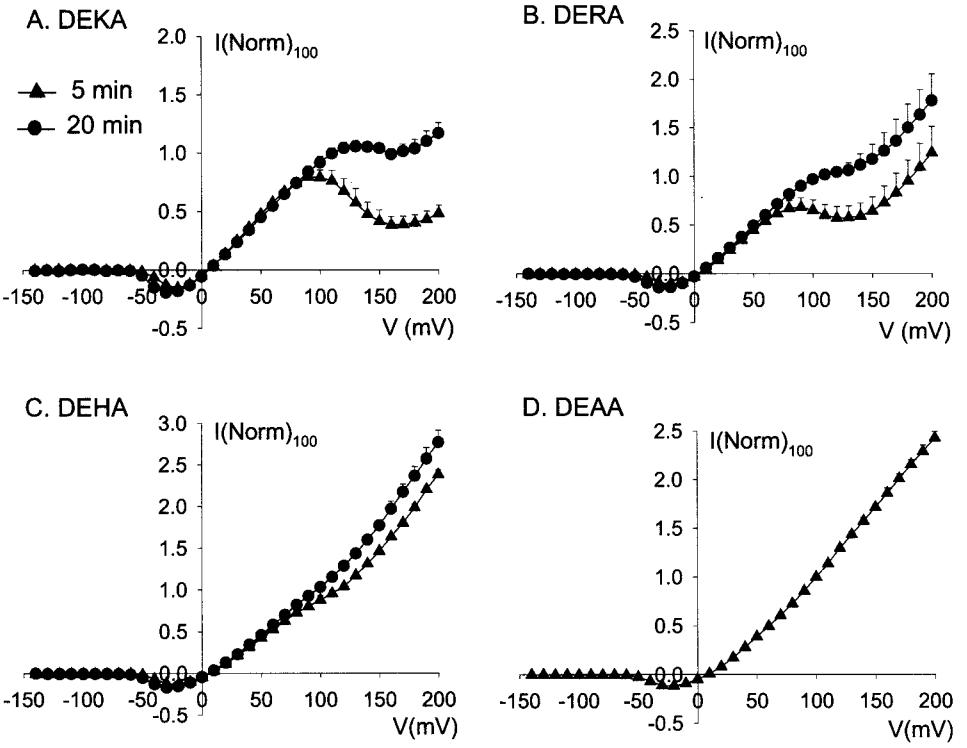

FIGURE 3 Comparison of whole-cell peak I-V behavior of the wild-type Na_V channel and various Lys(III) mutants in the presence of symmetrical 140 mM Na^+. (*A–D*) Whole-cell peak I-V relations of wild-type (DEKA), DERA, DEHA, and DEAA mutant channels recorded at 5 and 20 min after membrane break-in. Note that the DEAA mutant (*D*) displays nearly ohmic outward currents when measured immediately after establishing whole-cell configuration. Thus, only data collected at 5 min are shown for this particular mutant. I-V data points were normalized to the expected current at +100mV and averaged as the mean ± SE of 3 cells.

tylammonium (Huang et al., 2000). Permeability of the DEAA mutant to such large TAA^+ molecules is demonstrated by an upward inflection of the peak I-V curve at high positive voltage, a phenomenon that corresponds to relief-of-block due to voltage-driven permeation of a blocking cation outward through the channel (Huang et al., 2000). Fig. 3, *B* and *C*, shows behavior similar to that of large TAA^+ cations with respect to a positive inflection of the peak I-V curve and dependence on the residue substitution at the K(III) position. These observations thus support the idea that the phenomenon of endogenous block involves one or more substances that directly interact with the Na_V channel selectivity filter and are susceptible to voltage-driven permeation.

PAs such as spermidine and spermine induce complex I-V rectification behavior in wild-type and mutant Na_V channels

As mentioned in the Introduction, intracellular PAs are already known to block several major types of cation channel proteins. To investigate whether PAs may be responsible for endogenous blocking behavior in the rat muscle Na_V channel, we directly tested the effect of spermidine and spermine added to the pipette solution used for whole-cell recording. We found that these PAs produce complex I-V rectification that mimics several aspects of the endogenous blocking phenomenon.

Fig. 4 *A* compares four families of current responses to a standard voltage step protocol for HEK293 cells expressing the wild-type channel (DEKA) and three K(III) mutants (DERA, DEHA, DEAA). The whole-cell currents were obtained under conditions of symmetrical 140 mM Na^+ as in Fig. 3, except that 1 mM spermidine was added directly to the pipette solution. This concentration of spermidine produced I-V behavior that was quite stable within 5 min after membrane break-in, as if spermidine quickly equilibrates and overwhelms any time-dependent behavior produced by endogenous blocking substance(s).

Spermidine produced changes in the time course and peak value of outward currents as a function of positive voltage that are highly complex and differ for the various mutants (Fig. 4 *A*). We have not attempted to quantitate changes in the apparent time course of inactivation for outward currents of the various types of channels in the whole-cell configuration. In Fig. 4 *B* we focus instead on the peak I-V behavior. This figure shows that each type of channel displays a negative resistance region for peak outward current in the presence of 1 mM spermidine, however the voltage range of this effect and the negative slope of the peak current markedly depend on the particular mutant. Furthermore, the negative resistance region is followed by an upward inflection at higher positive voltage for DERA, DEHA, and DEAA mutants. By comparison, this latter upswing is practically absent for the wild-type channel at this concentration of spermidine (Fig. 4 *B*). Such behavior is consistent with a mechanism involving voltage-dependent

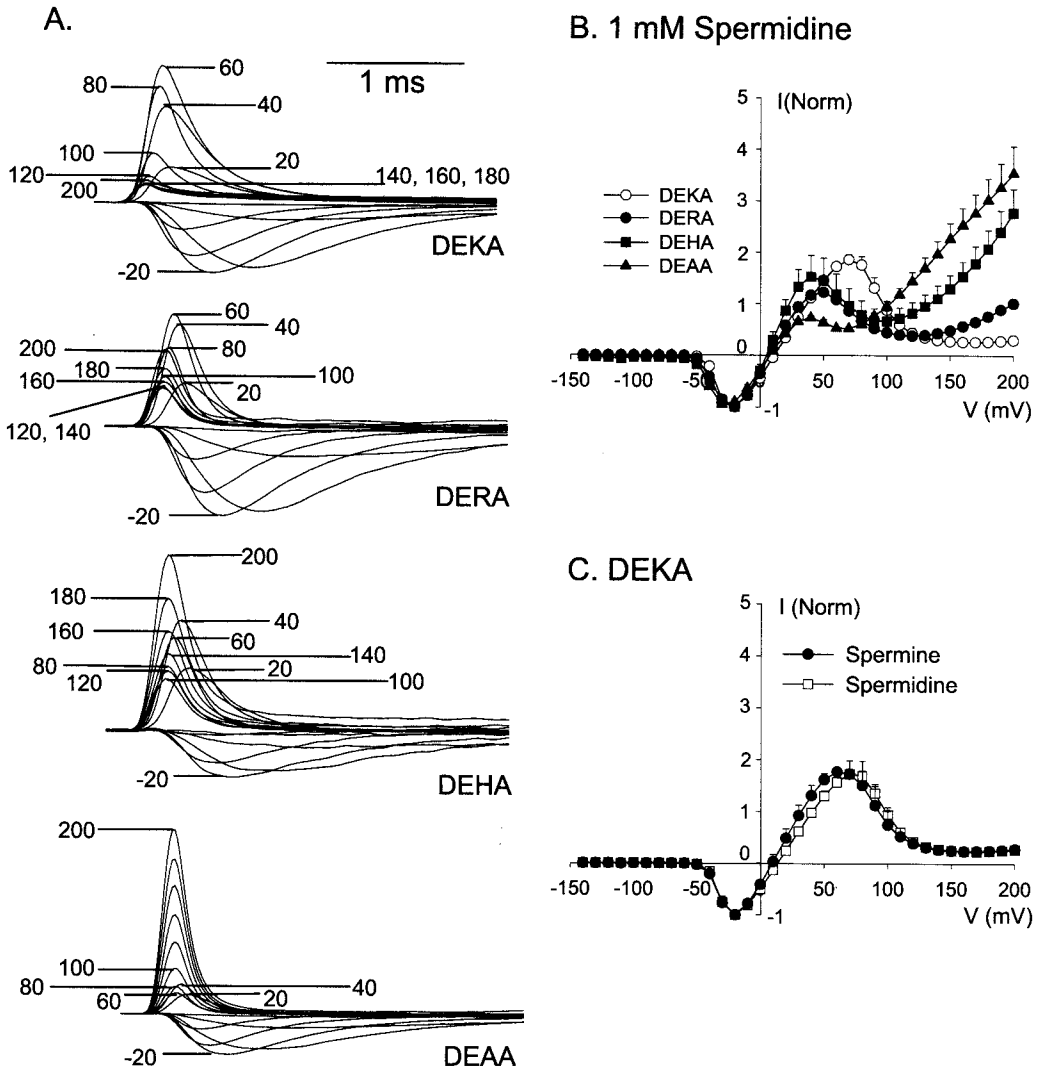

FIGURE 4 Effect of intracellular polyamines on whole-cell I-V behavior for the wild-type Na_V channel and various Lys(III) mutants under conditions of symmetrical 140 mM Na^+. (*A*) Comparison of whole-cell current traces of wild-type (DEKA), DERA, DEHA, and DEAA mutant Na_V channels in the presence of 1 mM spermidine in the pipette solution. The voltage pulse protocol was the same as in Fig. 1. For clarity, only traces at 20 mV increments of the step voltage from −120 mV are shown as labeled. The absolute magnitude of the maximum inward peak current was 7.5 nA (DEKA), 3.2 nA (DERA), 0.5 nA (DEHA), and 4.3 nA (DEAA). (*B*) Whole-cell peak I-V relations of wild-type (DEKA), DERA, DEHA, and DEAA mutants in the presence of 1 mM spermidine in the pipette solution. (C) Comparison of the effect of 1 mM spermine and 1 mM spermidine on whole-cell peak I-V relations of the wild-type Na_V channel. Data points in (*B*) and (*C*) are normalized to the maximum peak inward current and plotted as the mean ± SE for 3 to 5 cells.

block and relief-of-block by intracellular spermidine. The data of Fig. 4 *B* support the idea that relief-of-block by spermidine is facilitated by particular mutations of the K(III) residue that are known to destroy inorganic ion selectivity and increase the permeability of many organic cations as tested on the outside of the channel (Favre et al., 1996; Sun et al., 1997). The similarity between the effect of intracellular spermidine in the experiments of Fig. 4 *A* and the behavior of the endogenous rectification described in Figs. 2 and 3, suggests that intracellular PAs could mediate the latter phenomenon. Fig. 4 *C* compares the mean peak I-V relation for the wild-type channel in the presence of two different PAs added to the pipette solution, 1 mM spermidine, and 1 mM spermine. Data for these two molecules are nearly superimposable, implying that they have similar blocking behavior and that both types of cytoplasmic PAs could contribute to endogenous rectification.

Characterization of spermine and spermidine as permeant blockers in excised macropatches

Ultimately, one would like to know how intracellular PAs affect Na_V channel function in the cellular environment under physiological conditions. Before this can be determined, we believe it is important to elucidate basic features

of this ligand-channel interaction under well-defined ionic and biochemical conditions. To outline potential mechanisms that may be involved, in the remainder of this paper we present some key aspects of PA action on μ1 Na_V channels as tested on the cytoplasmic side of excised macropatches in the absence of cytosolic factors. Fig. 5 first describes the concentration dependence of the steady-state blocking effect of spermine and spermidine on peak outward current as measured by a voltage pulse from −120 to +100 mV for conditions of 140 mM symmetrical Na^+. The data are plotted as the ratio of peak current in the presence of PA to that for the same patch in the absence of PA. The concentration dependence of spermine and spermidine block in Fig. 5 represents equilibrium behavior since the results were not changed by decreasing pulse frequency at repetitive pulse intervals as long as 10 and 20 s. The blocking effect of these PAs on outward current is reversed by washing with bath perfusion for ~5 min as illustrated by the current records of Figs. 6 *A* and 7 *A*. The data of Fig. 5 *A* indicate that the equilibrium interaction of PAs with the wild-type (DEKA) channel is well described by a one-site binding isotherm with K_D values of 17 ± 3 μM for spermine and 35 ± 4 μM for spermidine. Fig. 5 *B* shows that the apparent blocking affinity of the DEAA mutant measured by the same method is quite similar to that of the wild-type channel with K_D values of 20 ± 1 μM for spermine and 66 ± 3 μM for spermidine.

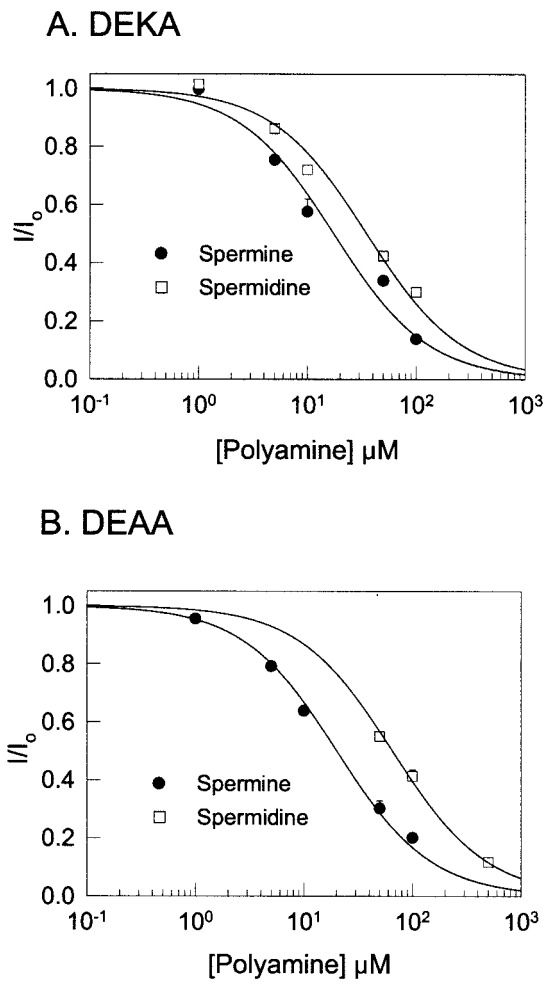

FIGURE 5 Concentration-dependent inhibition of wild-type (*A*) and DEAA mutant (*B*) Na_V current by spermine and spermidine. Outward Na_V current was evoked by 10-ms voltage pulses from −120 mV to +100 mV delivered once every 10 or 20 s under conditions of 140 mM symmetrical Na^+ in inside-out macropatches. The peak current was measured in the absence and presence of various concentrations of spermine or spermidine in the bath (cytoplasmic side). Data are plotted as the steady-state ratio (I/I_0) of peak current in the presence of PA to that in the absence of PA measured for the same patch. Data points represent the mean ± SE for at least 4 patches. Titrations are fit to $I/I_0 = K_D/([PA] + K_D)$ using best fit K_D values of 17 μM spermine (*A*), 35 μM spermidine (*A*), 20 μM spermine (*B*), and 66 μM spermidine (*B*).

Next we investigated the effect of PAs on the peak I-V relation in excised macropatches under conditions of symmetrical 140 mM Na^+ with the same pulse protocol used for the whole-cell experiments of Figs. 1 and 2. The goal of this experiment was to determine how the shape of the peak I-V relation varies with cytoplasmic PA concentration for wild type and DEAA channels. Fig. 6 *A* shows a family of wild-type macropatch currents evoked by a standard voltage step protocol before and after exposure to 100 μM spermine in the bath solution. As noted above, the strong inhibitory effect of spermine on outward current is substantially reversed by bath perfusion with a control solution. Fig. 6, *B* and *C*, shows average peak I-V curves taken in the absence and presence spermine and spermidine, respectively, at concentrations of 1, 5, 10, 50, and 100 μM. As discussed above for the similar peak I-V relations found in the whole-cell experiments of Figs. 2–4, these data exhibit concentration- and voltage-dependent I-V behavior that is characteristic of a permeant blocker. Such behavior has been documented for various inorganic and organic cation blockers in similar studies of many other types of ion channels (e.g., French and Wells, 1977; Sine and Steinbach, 1984; Blaustein and Finkelstein, 1990). The signature effect of such a blocking effect on the intracellular side is a negative resistance region in the I-V relation in the low positive voltage range, followed by a positive inflection or a relief-of-block at higher voltages.

A similar macropatch experiment for the DEAA mutant channel is presented in Fig. 7. These results show that spermine and spermidine inhibit outward currents through the mutant channel at similar concentrations that inhibit wild-type, but the apparent voltage dependence of block and relief-of-block is greatly altered. The negative-resistance region in the I-V curve is virtually absent. Instead, a weak inflection or plateau region is observed in the presence of these PAs in the low positive voltage range. Like their effect on the wild-type channel seen in Fig. 6, cytoplasmic PAs suppress outward current through the DEAA channel at low

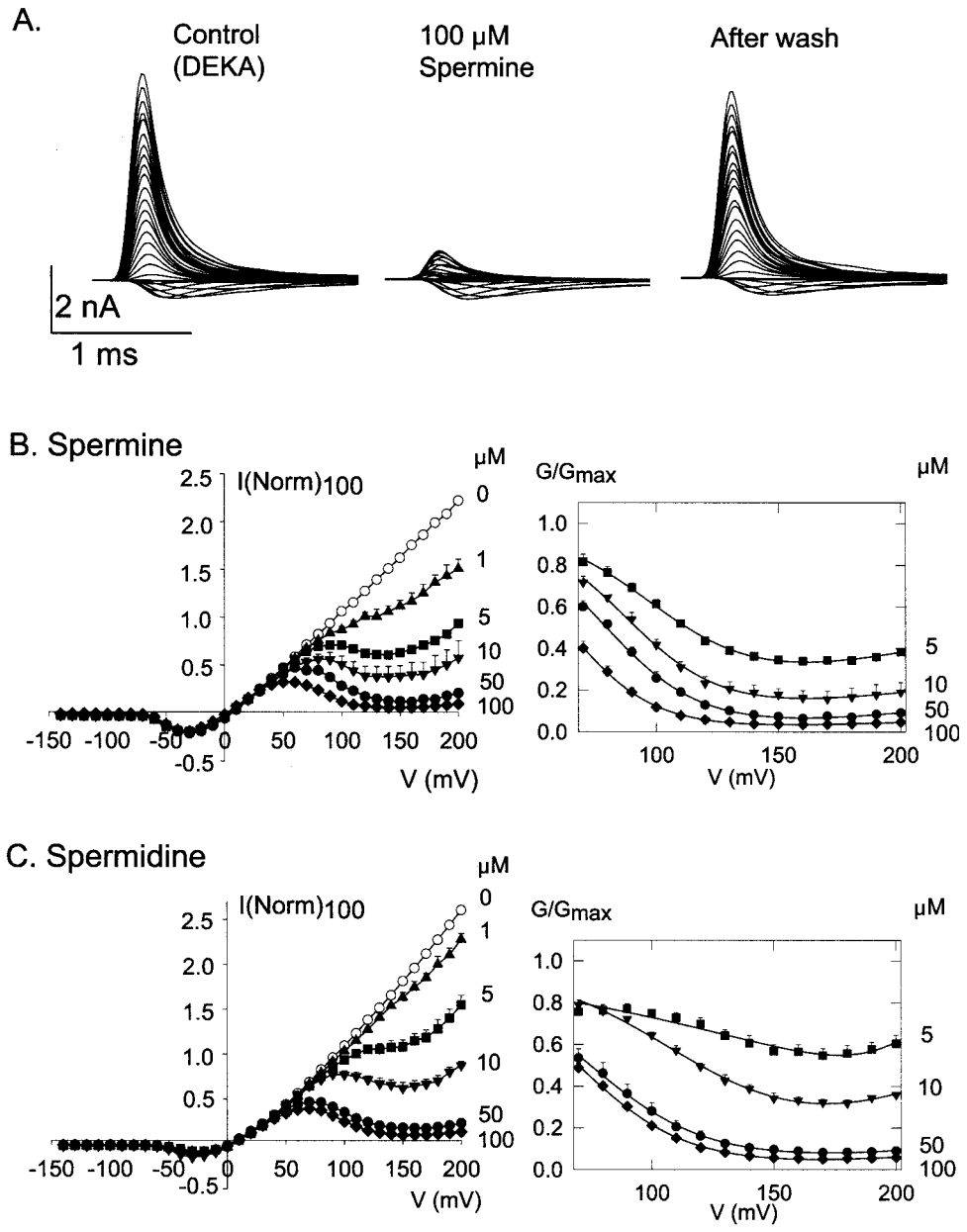

FIGURE 6 Effect of spermine and spermidine on wild-type Na_V channels in macropatches under conditions of symmetrical 140 mM Na^+. (*A*) Current records from a macropatch excised from an HEK293 cell expressing wild-type Na_V channels before, during, and after exposure to 100 μM spermine in the bath solution. (*B*) Effect of various concentrations of spermine on peak I-V relations of wild type Na_V channels in excised macropatches. (*left*) Peak I-V relations in the absence and presence of 1, 5, 10, 50, and 100 μM spermine in the bath solution. Data points are normalized to the peak current at +100 mV and plotted as the mean ± SE of 3 to 7 patches. (*right*) Corresponding normalized conductance-voltage relationships in the absence and presence of 5, 10, 50, and 100 μM of spermine. *Solid lines* are the best fit to a simple model of a permeant blocker as described in Materials and Methods. (*C*) Effect of spermidine on peak I-V relations of the wild-type Na_V channel in excised macropatches. Data handling and presentation follow those described in (*B*).

positive voltage, but there is a smoother conversion to ohmic behavior at voltages higher than +100 mV.

In an attempt to better understand the basis of the different I-V behavior of wild-type and DEAA channels in the presence of internal PAs, we fit the data to a simple model (Scheme 1) of a permeant blocker based on a single PA binding site, as described in the Materials and Methods section of this paper and in Huang et al. (2000) in more detail. Since the equilibrium dose-response relations for Na_V current inhibition by spermidine and spermine at a fixed voltage (Fig. 5) are well described by a one-site binding isotherm, this is the most economical model available to describe this system. In this analysis, we should caution that the I-V data of Figs. 6 and 7 do not necessarily represent equilibrium behavior at all potentials. This is because the I-V data were collected by consecutive pulses at intervals of 500 ms, a frequency (2 Hz) where use-dependent effects are present at some voltages (see Fig. 9). Nevertheless, the approximation of this situation by an equilibrium model is useful as a first-pass approach for investigating the basis for the dramatic difference in blocking behavior between the wild-type and mutant.

Normalized conductance-voltage relations were fit to Eq. 1, given in Materials and Methods. The right side of Fig. 6, *B* and *C*, shows such normalized conductance-voltage plots for 5, 10, 50, and 100 μM spermine and spermidine. In these plots, conductance is normalized to that from the same patch in the absence of PA. As indicated by the smooth

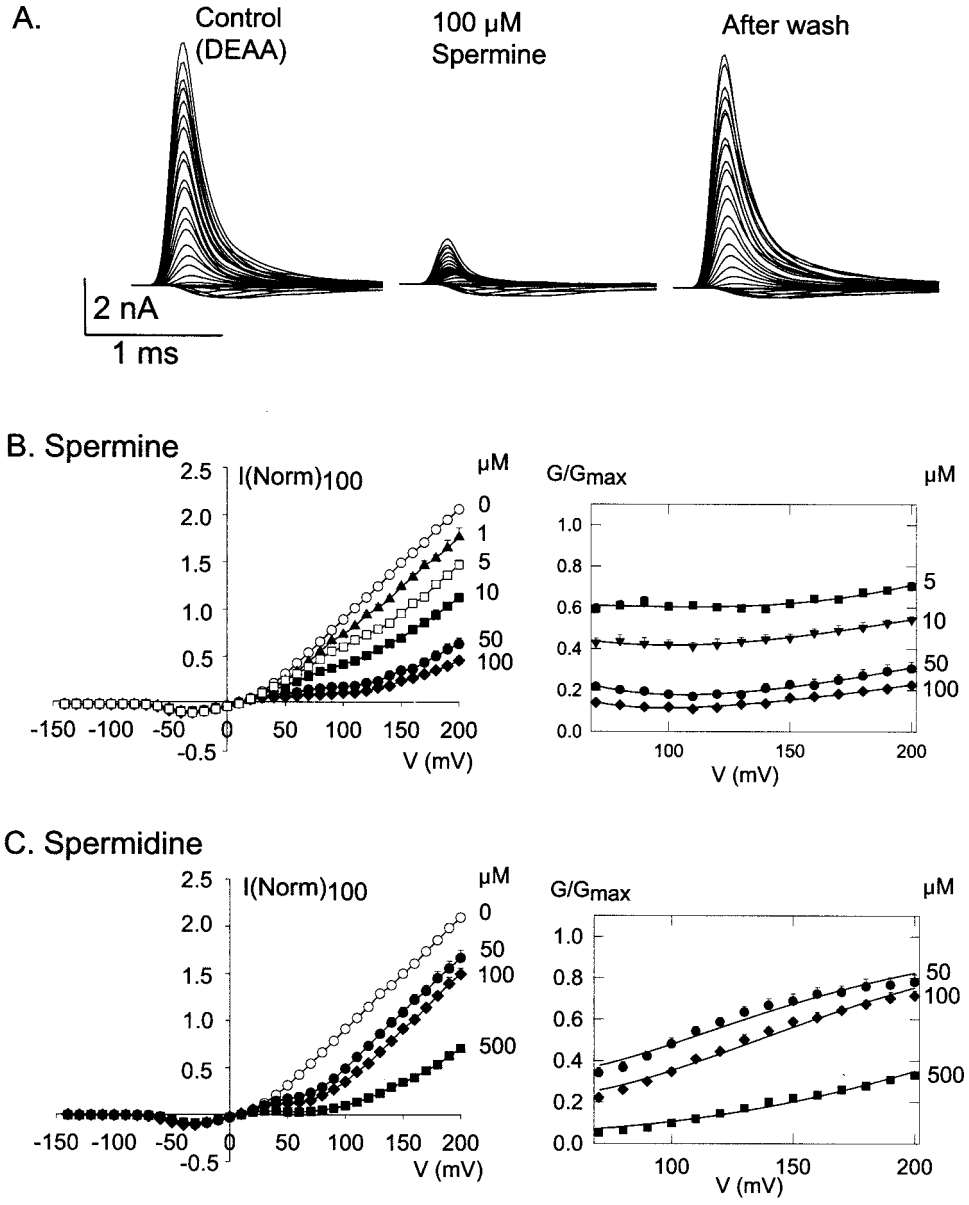

FIGURE 7 Effect of spermine and spermidine on DEAA mutant Na_V channels in macropatches under conditions of symmetrical 140 mM Na^+. (*A*) Current records from a macropatch excised from an HEK293 cell expressing DEAA mutant Na_V channels before, during, and after exposure to 100 μM spermine in the bath solution. (*B*) Effect of various concentrations of spermine on peak I-V relations of DEAA mutant channels in excised macropatches. (*left*) Peak I-V relations in the absence and presence of 1, 5, 10, 50, and 100 μM of spermine in the bath solution. Data points are normalized to the peak outward current at +100 mV and plotted as the mean ± SE for 3 to 7 patches. (*right*) Corresponding normalized conductance-voltage relationships in the absence and presence of 5, 10, 50, and 100 μM spermine. *Solid lines* are best fits to a simple model of a permeant blocker as described in Materials and Methods. (*C*) Effect of various concentrations of spermidine on peak I-V relations of DEAA mutant channels in excised macropatches. Data handling and presentation follow those described for (*B*).

curves, the simple theory is able to describe the wild-type data for PA block quite well. A comparison of best-fit parameters for 100 μM spermine and spermidine is shown in Table 1. The parameters indicate that the steep voltage dependence of block in the wild-type channel, which produces the negative resistance region, is derived from high values (1.1–1.4) of an effective electrical valence parameter, z'_1, that normally represents the product of the charge valence of the blocker and the fraction of transmembrane voltage sensed by the blocker (Woodhull, 1973). However,

TABLE 1 Parameters obtained by fitting conductance-voltage data in the presence of 100 μM spermine and spermidine to a simple model of permeant block

Channel type	Polyamine	$K_1(0)$ (mM)	z'_1	$K_R(0)$	z'_2
DEKA	spermine	3.5 ± 0.3	1.44 ± 0.03	$1.8 \pm 0.5 \times 10^{-4}$	1.69 ± 0.03
	spermidine	2.2 ± 0.3	1.13 ± 0.04	$1.6 \pm 1.2 \times 10^{-4}$	1.49 ± 0.09
DEAA	spermine	0.24 ± 0.21	1.21 ± 0.32	$160 \pm 130 \times 10^{-4}$	1.47 ± 0.31
	spermidine	0.47 ± 0.27	1.90 ± 0.43	$200 \pm 110 \times 10^{-4}$	2.34 ± 0.42

Normalized conductance-voltage data of Figs. 6 and 7 were fit to Eqs. 1–4. Best-fit parameters for 100 μM spermine and spermidine are shown along with standard errors derived from the fitting procedure.

it is difficult to interpret a physical distance from these parameters, since spermidine^{+3} and spermine^{+4} are long cationic molecules measuring 12.9 Å and 17.9 Å, respectively, in the linear extended conformation, and their charges are positioned over this length. The length of these molecules is also comparable to a large fraction of membrane bilayer thickness (~35 Å). Thus, the classic Woodhull (1973) blocking model, based on a point-charge located at a discrete binding site in the pore, does not apply well to this situation. Within the context of the model, it is interesting to note that the parameter, $K_R(0)$, the ratio of the dissociation rate constant for exiting the blocking site to the outside to that for exiting back to the cytoplasmic side at 0 mV, only needs to be in the range of $\sim 2 \times 10^{-4}$ (Table 1) in order to simulate voltage-dependent relief-of-block by these PAs for the wild-type Na_V channel.

The same model for permeant block can also describe the peak I-V behavior of the DEAA mutant as shown by fits of the normalized conductance-voltage data on the right side of Fig. 7, *A* and *B*. Comparison of the best-fit model parameters for DEKA and DEAA listed in Table 1 shows that the I-V behavior of the DEAA mutant versus wild-type can be largely explained by a ~100-fold increase in $K_R(0)$, the ratio of rate constants for blocker dissociation to the outside versus inside at 0 mV. The effect of the DEAA mutation on block by internal PAs is, therefore, rather similar to that previously described for block by large TAA^+ molecules (Huang et al., 2000). In both cases, mutation of the selectivity filter Lys(III) residue to Ala greatly enhances relief-of-block and outward permeation of particular types of large organic cations.

Effect of PAs on the macroscopic time course of inactivation and use dependence of PA block

Many compounds that block Na_V channels from the internal side have also been found to interact with the inactivation gating process and alter its time course (Armstrong and Croop, 1982; Cahalan and Almers, 1979; Yeh and Narahashi, 1977; O'Leary and Horn, 1994; O'Leary et al., 1994). Fig. 8 summarizes effects of spermine and spermidine on

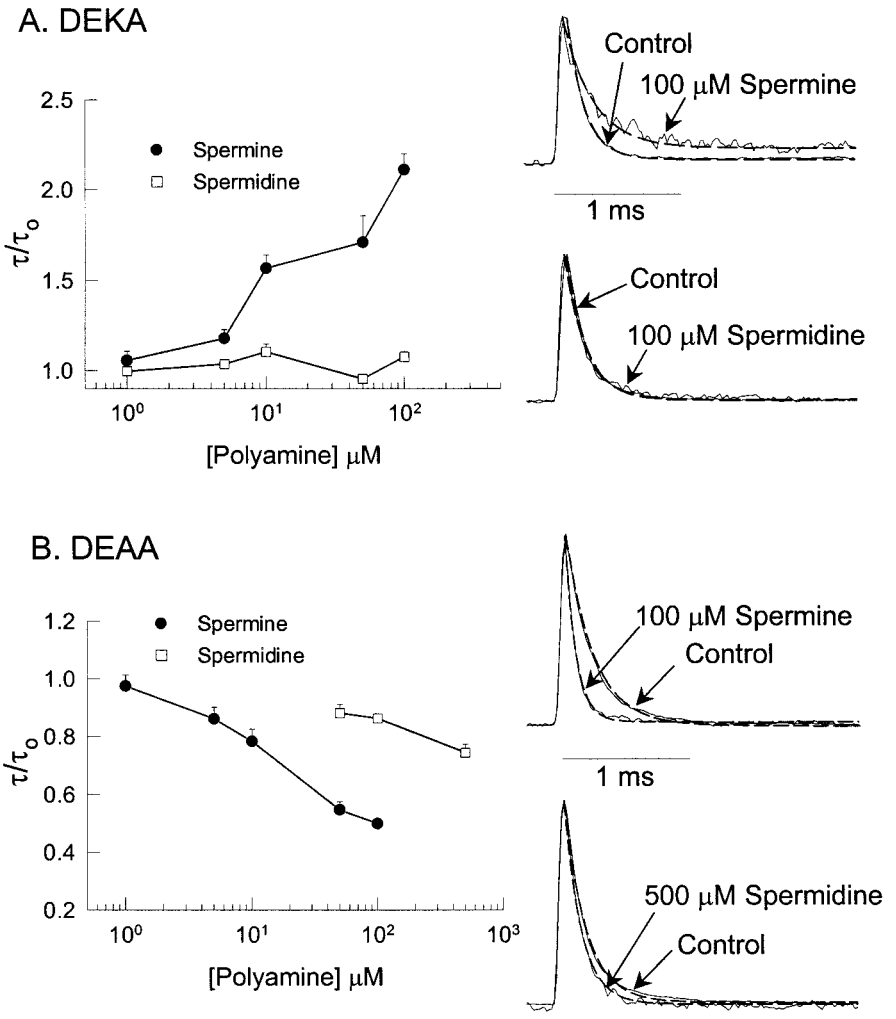

FIGURE 8 Effect of spermine and spermidine on the macroscopic time course of inactivation for wild-type (*A*) and DEAA mutant (*B*) Na_V channel current. Outward current was measured in macropatches under conditions of symmetrical 140 mM Na^+. The voltage pulse protocol was the same as described for Fig. 5 (single pulses from −120 mV to +100 mV every 10 or 20 s). Typical records at the right show 70–90% inhibited Na_V current in the presence of PA superimposed on control current in the absence of PA and scaled so that peak current values coincide. *Dashed lines* show typical fits of the inactivation time course to a single exponential function of time. Plots at the left show the ratio of inactivation time constants in the presence of spermine or spermidine to that in the absence of PA. Data points represent the mean ± SE for at least 4 patches. *Solid lines* are used to connect data points.

the macroscopic time course of inactivation for outward current elicited by a voltage step from −120 to +100 mV in excised macropatches studied in the presence of symmetrical 140 mM Na^+. This data was obtained from the same equilibrium titration measurements of block in Fig. 5 and thus represent the response of channels that have achieved steady state inhibition of peak current as determined by a constant response to repetitive pulses delivered at long intervals of 10 or 20 s. To measure the apparent inactivation rate, τ_i, we fit the time course of current decay to a single exponential in the absence and presence of spermine or spermidine. As illustrated by the current traces of Fig. 8, the inactivation time course is well described by a single exponential under all conditions. Scaling of the peak of inhibited (70–90%) current measured in the presence of 100 μM spermine or spermidine onto the peak of control current in the absence of PAs demonstrates that these ligands can either increase or decrease τ_i, depending on the K(III) residue. Specifically, spermine increased τ_i by greater than twofold for the wild-type channel in a concentration-dependent manner, but spermidine had no significant effect on τ_i (Fig. 8 *A*). In contrast, both spermine and spermidine decreased τ_i for the DEAA mutant as a function of increasing concentration (Fig. 8 *B*).

Both lengthening and shortening effects of blockers on the time course of inactivation have been previously described for voltage-gated ion channels. For example, internal tetraethylammonium was found to block the Shaker K_V channel and prolong N-type inactivation (Choi et al., 1991). This latter effect was interpreted as a strictly competitive interaction between the blocker and the inactivation particle. By analogy, a possible interpretation of the lengthening effect of spermine on inactivation of the wild-type Na_V channel is that this molecule prevents binding of the Na_V channel inactivation gate to its receptor site, a process that is proposed to correspond to binding of the "hinged lid" or IFM motif in the Domain III-IV linker (Catterall, 2000; Eaholz et al., 1999). It is interesting that the shorter spermidine molecule does not produce this lengthening effect under the tested conditions (Fig. 8 *A*). A possible interpretation is that bound spermidine lodges deeper in the pore so as not to occlude binding of the hinged lid, whereas spermine is long enough (17.9 Å) to interfere physically with this process. In contrast, spermine and spermidine both shorten the apparent inactivation rate of the DEAA mutant (Fig. 8 *B*). Such a concentration-dependent shortening effect is thought to reflect primarily a rapid bimolecular association rate (k_{on}) of blockers to the open channel and is manifested when the intrinsic blocker dissociation rate (k_{off}) is slow compared to inactivation (O'Leary et al., 1994). In the present case, enhanced outward permeability of PAs through the DEAA channel (Fig. 7) could also account for the shortening of τ_i in DEAA versus lengthening of τ_i in the wild-type channel.

Because spermine and spermidine are hydrophobic cations that block the rat muscle Na_V channel from the cytoplasmic side, we investigated whether they exhibit use dependence. Use dependence is a phenomenon associated with many types of LA drugs typified by hydrophobic tertiary amines, such as lidocaine (Hille, 1992). The charged form of LAs is known to preferentially block Na_V channels from the cytoplasmic side (Strichartz, 1973). Use dependence of LAs is typically monitored by delivering a series of repetitive depolarizing pulses and recording the time-dependent decline in peak Na_V current amplitude.

Fig. 9 summarizes use-dependent activity of spermidine and spermine as observed in macropatch experiments with wild-type and DEAA mutant Na_V channels under conditions of symmetrical 140 mM Na^+. In the top panels of Fig. 9, *A* and *B*, outward Na_V currents were evoked by repetitive pulses at a frequency of 4 Hz to +150 mV (3.25 ms in duration) from a holding potential of −120 mV in the absence or presence of PAs. The peak outward current was normalized with respect to the amplitude of the first pulse; i.e., the control current value in the absence of PA or the tonic (first pulse) level of inhibited current in the presence of PA. Under these conditions, the wild-type channel displayed rapid time-dependent inhibition in the presence of spermine and spermidine. In experiments of Fig. 9 *A*, phasic enhancement of block by repetitive stimulation amounted to ~44% by 20 μM spermidine and ~29% by 10 μM spermine. This effect is not simply due to an accumulation of rapid inactivation, since control currents measured in the absence of PAs exhibit only a slight decline during 50 s exposure to the same stimulation protocol (Fig. 9). The kinetics and amplitude of extra block depend on the frequency of stimulation and the concentration of spermine and spermidine (not shown), properties similar to the action of use-dependent LA drugs (Hille, 1992). The lower panels in Fig. 9 show that the fractional amplitude of extra-block induced by phasic stimulation is also highly dependent on the voltage of the step depolarization. This is to be expected, since equilibrium occupancy of the channel by PAs is governed by competing processes of block and relief-of-block in the positive voltage range. Another observation is that the kinetics of use dependence are affected by mutation of the selectivity filter Lys(III) residue. Fig. 9 *B* (top) shows that the DEAA mutant displays a considerably slower time course of phasic inhibition for spermine (τ = 1.4 s for the major time constant of the relaxation) and spermidine (τ = 2.3 s) as compared to the wild-type channel ($\tau < 0.4$ s for both PAs in Fig. 9 *A*). Fig. 9 *B* (bottom) shows that use dependence of block of the DEAA mutant by 10 μM spermine exhibits a biphasic dependence on test potential in the range of +50 to +200 mV, with maximum extra block occurring at +100 mV. In contrast, use-dependent extra block of the DEAA mutant by 50 μM spermidine was greatest at +150 mV. These findings indicate that use-dependent inhibition by PAs depends on the structure of the

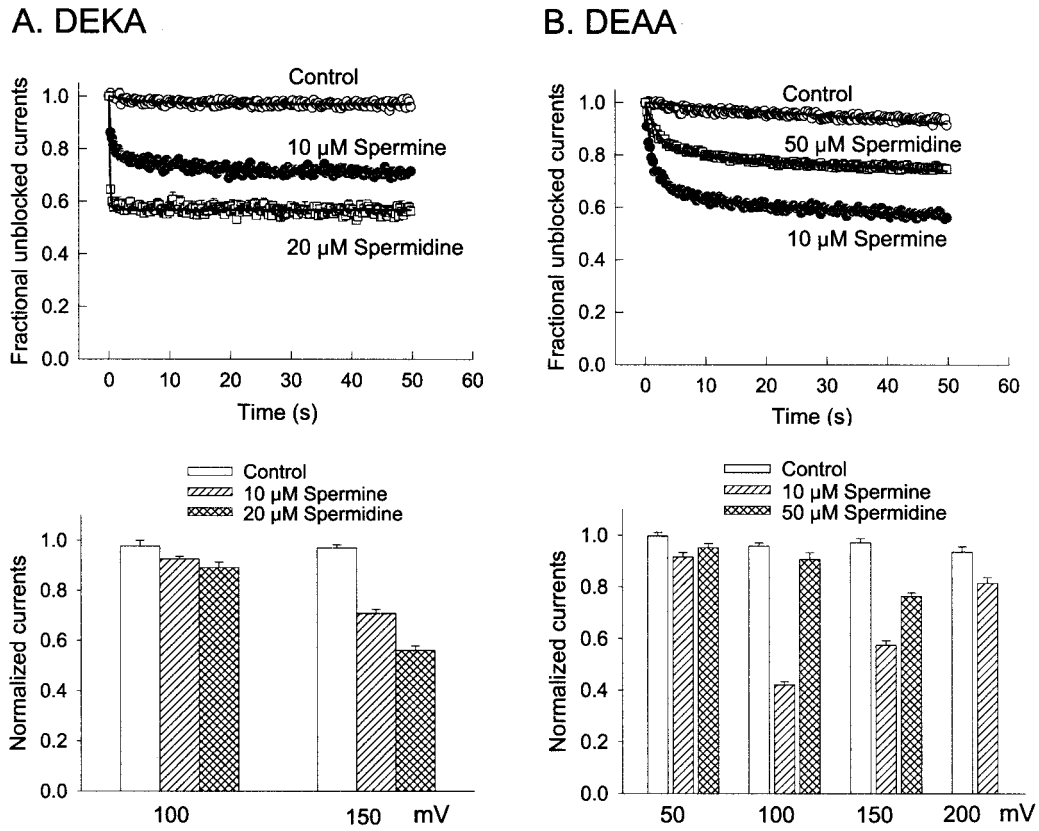

FIGURE 9 Use-dependent behavior of polyamine block of wild-type and DEAA mutant Na_V channels as measured in excised macropatches in the presence of symmetrical 140 mM Na^+. (*A*) Wild-type channel. (*top*) Fractional unblocked peak currents were measured with a repetitive train of 3.25-ms pulses to +150 mV from a holding potential of −120 mV at a frequency of 4 Hz. Data points were normalized to the first response of the test pulse and plotted as the mean ± SE for 3 to 10 patches. *Solid lines* are the best fit to a sum-of-two exponential function. (*bottom*) Voltage-dependent variation of the fractional extra block by spermine and spermidine for the wild-type channel. Bars represent the fraction of unblocked current averaged from the last 5 s of data recorded with trains of 4-Hz pulses to +100 or +150 mV, in the absence and presence of 10 μM spermine or 20 μM spermidine in the bath solution as indicated. Data are normalized to the first pulse and represent the mean ± SE for 3 to 10 patches. (*B*) DEAA mutant channel. (*top*) Fractional unblocked peak currents measured as described in (*A*). Data handling and presentation follow those described in (*A*).

PA molecule as well as the detailed kinetics and voltage dependence of block and unblock by these inhibitors.

Effect of spermine on voltage-dependent gating

The effects of PAs described so far pertain to nonphysiological conditions of high internal Na^+ concentration. Internal Na^+ may compete for occupancy of the pore or otherwise affect interactions of PAs with the channel. To examine PA-channel interactions in the presence of a near-physiological Na^+/K^+ gradient, we tested the effect of spermine using excised inside-out macropatches with 140 mM Na^+/3 mM K^+ in the pipette (outside) solution and 135 mM K^+/3 mM Na^+ in the bath (inside) solution. Under these conditions, the peak current of the wild-type channel reverses near +80 mV due to high selectivity for Na^+ versus K^+. Addition of spermine (1 mM) to the bath solution completely blocks outward current under these conditions and inhibits peak inward current by 36% (Fig. 10 *A*). The apparent rate of rapid inactivation of residual inward current in the presence of spermine is not significantly altered. The current traces labeled "after wash" in Fig. 10 *A* were recorded after extensive perfusion of the patch with control bath solution. Blocked outward current recovered to 91% of control, whereas the maximum inward current consistently recovered to only ~70% of control. Peak I-V data of Fig. 10 *B* also shows that a smaller fraction of inward vs. outward current is recovered after exposure to spermine. This latter behavior suggests that the blocking effect of spermine at positive voltage is distinct from its effects on channel gating and may indicate multiple sites of PA action. For example, PA polycations could adsorb to phospholipids or other negatively charged sites on the exposed intracellular membrane surface and thereby exert electrostatic or allosteric effects on Na_V channel gating independently of blocking interactions that occur by binding of PAs within the pore. Fig. 10 *B* shows that spermine does not affect ionic selectivity, since it does not change the reversal potential.

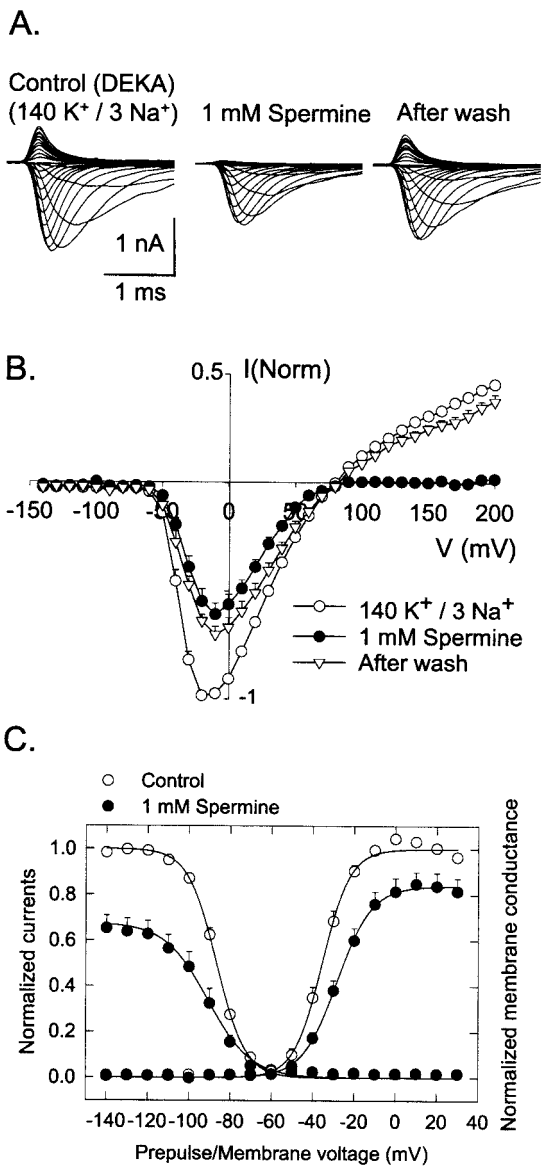

FIGURE 10 Spermine inhibits inward current and shifts the voltage dependence of gating of wild-type Na_V channels as recorded in macropatches with a physiological Na^+/K^+ gradient. (*A*) Representative current traces recorded from a macropatch excised from an HEK293 cell expressing wild-type Na_V channels in a control solution containing of 140 Na^+/3 mM K^+ in the pipette solution and 135 mM K^+/3 mM Na^+ in the bath solution. Records are shown before, during, and after exposure to 1 mM spermine in the bath solution, as indicated. (*B*) Peak I-V relations of wild-type Na_V channel for the experimental conditions described in (*A*). Data points are the mean ± SE for 5 to 7 patches and are normalized to the maximum peak inward currents from the same patch before exposure to spermine. (*C*) Normalized steady-state Na_V channel availability and normalized membrane conductance as a function of prepulse and step potentials, respectively, measured in the absence and presence of 1 mM intracellular spermine in the bath solution. Steady-state availability was measured from the peak currents elicited by a test pulse to −10 mV applied directly after a 250-ms conditioning pulse at the indicated membrane potentials ranging from −140 mV to +30 mV, with pulses delivered at intervals of 0.5 s. Normalized membrane conductance was computed from data in (*B*). Data points are the mean ± SE for 4 cells (availability) or 7 cells (conductance). Steady-state availability data were fit to the following transform of a Boltzmann function: $I/I_{max} = \{1 + \exp[(V - V_{0.5})/k]\}^{-1}$, where V is the prepulse potential, $V_{0.5}$ is the voltage for half-inactivation, and k is a slope factor. The best-fit values are: $V_{0.5} = -86.6 \pm 0.6$ mV, $k = 7.1 \pm 0.4$ mV for control, and $V_{0.5} = -93.7 \pm 1.0$ mV, $k = 9.3 \pm 0.8$ mV for 1 mM spermine. Conductance activation data were fit to the same Boltzmann transform, where V is the test potential, $V_{0.5}$ is the voltage for half-activation, and k is a slope factor. The best-fit values are $V_{0.5} = -35.5 \pm 1.5$ mV, $k = -6.6 \pm 0.2$ mV for control, and $V_{0.5} = -28.2 \pm 1.4$ mV, $k = -8.5 \pm 0.5$ mV for 1 mM spermine. Spermine-dependent shifts of the midpoint voltage ($V_{0.5}$) for availability and relative conductance are significantly different ($P < 0.05$) as determined by an unpaired *t*-test.

Analysis of the availability-voltage relationship for Na_V channel inactivation (Fig. 10 *C*) indicates that 1 mM spermine stabilizes channels in the inactivated state by significantly shifting the midpoint of the availability curve by −7.1 mV ($V_{0.5} = -86.6 \pm 0.6$ mV vs. -93.7 ± 1.0 mV for control vs. spermine, see Fig. 10 legend). The macroscopic conductance-voltage relationship for Na_V channel activation is also significantly affected by spermine with an apparent shift of +7.3 mV for the midpoint of voltage-dependent activation (Fig. 10 *C*). Both effects of spermine would act to decrease the probability of Na_V channel opening under physiological conditions. In summary, the results of Fig. 10 indicate that 1 mM internal spermine has significant effects on Na_V channel activity in the physiological range of membrane voltage under cellular ionic conditions.

DISCUSSION

In this study, we describe a phenomenon involving anomalous rectification of whole-cell outward current mediated by the rat muscle Na_V channel. This behavior was observed in a heterologous human cell line, HEK293, that is commonly used for expression of cloned channel proteins. The use of Na^+ as the principal intracellular cation is a salient condition of this experiment, in that it carries a large outward current and reveals the presence of an endogenous cellular blocking activity that would otherwise be masked within the small outward current of a less permeant ionic species such as Cs^+ or K^+. The absence of divalent cations such as Mg^{2+} and Ca^{2+} in the pipette solution eliminates from consideration the known intracellular blocking activity of divalent metal cations (Pusch, 1990) as possible mediators of this anomalous rectification. Our finding of endogenous inward rectification of Na_V channels in a fibroblast-like cell line under conditions of symmetrical [Na^+] may be juxtaposed with classical observations of inward current rectification of K_{IR} channels, where the original description, "anomalous" rectification (Katz, 1949), was based on the fact that little outward K^+ current is observed under conditions where a K^+-selective pore is expected to pass a large outward current; i.e., for cytoplasm containing high intracellular K^+.

Since the discovery that intracellular PAs are largely responsible for inward rectification of K_{IR} channels (Ficker et al., 1994; Lopatin et al., 1994), many other types of ion channels have been found to be blocked or modulated by this class of cytoplasmic organic cations (Williams, 1997). Our observations on the effect of spermidine and spermine add Na_V channels to the growing list of cation-selective channels that exhibit significant interactions with PAs. In connection with this phenomenon, it should be noted that related observations have been previously described for the human heart Na_V channel isoform (Townsend et al., 1997; Townsend and Horn, 1999). These latter studies showed that this Na_V channel expressed in the tsA201 cell line exhibits a sublinear peak I-V relationship of outward current in the range of 0 to +70 mV in the presence of high internal Na^+ and a poorly permeant external cation such as Cs^+ or N-methyl-D-glucamine. Similar to our findings, this latter interaction was greatly attenuated by the K1418C mutation of the selectivity filter Lys residue and was proposed to be caused either by a fast gating mechanism or block by an endogenous polyvalent cation such as spermine (Townsend and Horn, 1999).

The present work does not identify which intracellular PAs or other such molecules are the exact cause of rectification in the whole-cell experiments of Fig. 2. A precise identification would require chemical fractionation of the cytoplasm of HEK293 cells, isolation of compounds that produce intracellular block, and structural confirmation that such compounds are indeed PAs. Furthermore, endogenous block may be due to a mixture of endogenous compounds that interact with the Na_V channel and other cellular constituents (e.g., nucleic acids, nucleotides, and phospholipids) in a system of great complexity. Results with excised patches do unequivocally show that spermine and spermidine produce blocking and I-V behavior (Figs. 6 and 7) that mimic the endogenous rectification phenomenon seen in whole cells (Figs. 2 and 3). This correlation includes mechanistic details such as N-shaped peak I-V relations attributed to voltage-dependent block and relief-of-block, and the special behavior of several selectivity filter mutants (DERA, DEHA, DEAA), which greatly enhance relief-of-block. Because spermine and spermidine are undoubtedly present in HEK293 cells, we can infer that these PAs are likely candidates for the endogenous blocking molecule(s), but we cannot exclude the possibility that other endogenous substances also play a role.

Although it is known that PAs are present in the cytoplasm of all cells (Igarashi and Kashiwagi, 2000), the exact concentration of spermine and spermidine in the vicinity of the plasma membrane is difficult to ascertain. The total cellular concentration of PAs has been stated to lie within the wide range from 10 μM to 10 mM (Nichols and Lopatin, 1997), but the relevant free concentration is governed by extensive binding of PAs to intracellular polyanions and anionic surfaces such as ATP, RNA, DNA, and phospholipid. Based on a quantitative model of such binding, the free concentration of spermidine and spermine in a bovine lymphocyte has been estimated at 200 and 80 μM, respectively (Igarashi and Kashiwagi, 2000). For rat hepatocytes, the latter reference estimates values of 80 μM free spermidine and 20 μM free spermine. To address this issue here, we used PA inhibition of the rat muscle Na_V channel measured in excised macropatches (e.g., Fig. 5) to calibrate and estimate the effective concentration of spermidine and spermidine that would produce the observed level of endogenous inhibition at ~0.2 min after whole cell break-in (e.g., Fig. 2 *A*). We performed such a calibration at three different voltages (+100, +150, and +200 mV) and used the observed inhibition relative to ohmic behavior to calculate the effective concentration of PAs. This analysis indicates that the endogenous inhibition of outward Na_V current at an early time after break-in could be produced by intracellular spermidine in the range of 91 to 132 μM or by intracellular spermine in the range of 40 to 43 μM. These values are similar to the estimated values of free PAs present in cultured lymphocytes and hepatocytes (Igarashi and Kashiwagi, 2000).

Another interesting aspect of the endogenous rectification phenomenon is the slow rate of conversion (i.e., $\tau = 22$ min, Fig. 2 *C*) of outward Na_V channel current to ohmic behavior in whole-cell recording. Since molecules as small as spermine and spermidine are expected to equilibrate in less than one minute for cell-pipette dilution based on simple diffusion (Marty and Neher, 1995), we infer that some unspecified process restricts the release of cytoplasmic PAs from HEK293 cells. A possible mechanism to explain such behavior is that an intracellular reservoir containing PAs may slowly leak or transport these molecules to the cytoplasmic compartment. One scenario that can be imagined is slow release from a compartmentalized pool of PAs followed by surface adsorption to proteins and lipids. In fact, recent studies suggest that PAs in mammalian cells are concentrated within vesicular endosome-like compartments as visualized by confocal laser scanning microscopy and fluorescent PA analogues (Cullis et al., 1999). Aside from its potential biological significance, this slow equilibration also has implications for electrophysiological studies of Na_V channels and potentially other types of ion channels in mammalian cell lines. In particular, the interpretation of whole-cell I-V behavior in studies of ion permeation and gating, particularly within the first 20 min after membrane break-in, may be subject to potential complications of time-dependent changes in block due to equilibrating PAs.

The behavior of the K(III) mutants (DERA, DEHA, DEAA) with respect to the PA blocking interaction provides new information related to the role of the Na_V channel selectivity filter in ion permeation and molecular sieving of organic cations. The data of Figs. 4, 6, and 7 show that the efficiency of relief-of-block by intracellular spermidine and spermine clearly varies with the chemical nature of the

amino acid side chain substituted at the K(III) position of the DEKA locus. As mentioned in the Introduction, the DEKA locus is a set of mostly charged residues in homologous Domains I-IV that play a major role in determining ionic selectivity in Na_V channels. The fact that such K(III) mutations strongly affect relief-of-block behavior supports the idea that the positively charged Lys side chain at this position in the native Na_V channel faces the pore lumen and interacts with organic cation blocker molecules entering the channel from the internal side.

Since spermine, a long linear molecule with approximate cylindrical dimensions of 4.6 Å (diameter) × 17.9 Å (length), is amenable to relief-of-block in the wild-type Na_V channel, it is evident that the native selectivity filter is able to accommodate the voltage-driven passage of certain linear alkylammonium cations that enter the channel from the inside. In contrast, permeation of organic cations such as methylammonium and ethylammonium is not detected when such molecules are tested as current carriers from the extracellular side of the channel (Hille, 1971; Sun et al., 1997). These observations are not necessarily incompatible. An indirect assay for permeation based on relief-of-block is much more sensitive than measurements of current carried by a test cation. The relief-of-block assay allows one to observe dramatic changes in the shape of an I-V curve due to movement of a blocking ion through the channel at rates less than 0.1% of a highly permeant ion such as Na^+. The cylindrical diameter of spermine (4.6 Å) is close to the cutoff dimensions of ~3 Å × ~5 Å estimated for the cross-sectional area of the narrowest region of the Na_V channel pore (Hille, 1971), a region now closely identified with the DEKA locus (Sun et al., 1997). One only has to postulate that the K(III) side chain is capable of being displaced or swinging out of the way when PAs pass through this narrow region of the pore, driven by high positive voltage. This type of organic cation permeation through the Na_V channel leads to the picture of a long worm-like molecule (spermine) sliding through a molecular nanotube that has one major site of constriction situated close to the outside of the membrane. Besides movement of the side chain of Lys(III) and possibly other residues that form the filter region, it is also possible that this region undergoes a more radical type of transient deformation to accommodate permeation of PA cations. For example, the PA cation might also dissociate from its blocking site to the outside by intercalating into one of the contact regions between the four pseudo-subunit domains, essentially sliding through a crack in the Na_V channel protein. We recently proposed a similar idea to explain how certain large tetraalkylammonium cations such as tetrapentylammonium exhibit relief-of-block behavior (Huang et al., 2000).

In comparing the phenomenology of PA blocking interactions observed here with that previously described for K_{IR}, GluR, AchR, and CNG channels (Lopatin et al., 1995; Lu and Ding, 1999; Bähring et al., 1997; Haghighi and Cooper, 2000), one is struck by the fact that different types of channel pores vary greatly in affinity, stoichiometry, and voltage dependence of block and relief-of-block for spermine and spermidine. It is clear that simple PA molecules engage in a diverse variety of specific chemical interactions with channel proteins that presumably reflect important differences in channel architecture and physiological function. However, a common structural theme that has clearly emerged from studies of PA block is that many different cation channels contain a site in the permeation path, closely associated with negatively or positively charged amino acid residues (e.g., K(III) in the Na_V channel), that control both Ca^{2+}/Mg^{2+} permeability/block and PA block (Taglialatela et al., 1995; Yang et al., 1995; Lu and MacKinnon, 1994; Haghighi and Cooper, 2000; Williams, 1997).

Although chemical and structural similarity between PA molecules and typical LA drugs such as lidocaine extends only as far as the presence of amine functional groups and hydrophobic moieties, this study finds evidence of a common mode of action on the rat muscle Na_V channel. Both types of molecules preferentially block the open channel from the intracellular side, bind to the channel in a voltage-dependent fashion favored by depolarization, exhibit stimulus-dependent binding (i.e., use dependence), interact with inactivation gating, and produce negative shifts of steady-state availability (a measure of rapid inactivation). These functional similarities are likely to result from common or overlapping binding sites for PAs and LAs on the Na_V channel protein. Residues critical for high-affinity binding of LAs have been mapped to the S6 transmembrane segment of Domain IV (Ragsdale et al., 1994; Catterall, 2000), a region that is believed to form a hydrophobic α-helix that forms part of the intracellular lining of the pore. Based on current models of Na_V channel structure, it is believed that LA molecules enter the intracellular portion of the ion permeation pathway, physically occlude passage of Na^+, and somehow interact with the fast-inactivation gating process to produce use-dependent inhibition (Catterall, 2000; Scheuer, 1999). Results presented in this paper support the idea that spermine and spermidine bind within the same region of the Na_V channel as LAs and traverse to the outside by electrodiffusion after passing through a major physical barrier at the selectivity filter. This leads to the prediction that binding competition is likely to occur between endogenous PA molecules and LAs. If a PA molecule and an LA molecule can simultaneously bind to the channel, there may also be electrostatic or allosteric binding interactions between these two types of ligands. Such binding interactions could have clinical implications for the use of LA drugs. For example, if cellular PA concentrations differ among excitable tissues or undergo changes in disease states, LA-type drugs could be rendered less or more effective, depending on the circumstances.

From a broader standpoint, the present results lead us to consider whether PA interactions represent a significant

mechanism of Na_V channel modulation under physiological conditions. The most prominent effect of spermine and spermidine described here is a strong voltage-dependent block in the positive voltage range greater than +50 mV. At first glance, it might be supposed that this effect is unlikely to affect the shape or frequency of action potentials, since excitable cells are rarely depolarized to voltages greater than +50 mV. However, in cells with a substantial contingent of Na_V and Ca_V channels (e.g., cardiac cells and neurons), block of Na_V channels could potentially affect the slope of the rising phase and the amplitude of action potentials by limiting the contribution of Na^+ conductance. In principle, there may be situations where the membrane potential would be rapidly driven to high values unless its rising trajectory is limited by PA block of Na_V channels. By this mechanism, intracellular PAs could act as a safety device to suppress excessive Na^+ conductance during rapid depolarization. Aside from voltage-dependent block, the results in Fig. 10 indicate that there are also inhibitory effects of PAs on inward Na^+ current in the negative and low positive voltage range where cellular electrical activity normally occurs. Such effects on Na_V channel inactivation or activation are potentially of greater functional significance than voltage-dependent block. Another unexplored issue concerns isoform specificity. Isoform-dependent interactions with spermine and spermidine are already known to occur for the K_{IR} and GluR families of ion channels (Williams, 1997), and it is possible that neuronal or heart isoforms of Na_V channels may respond to PAs differently than the muscle subtype studied here. In closing, it seems that our initial look at the effect of intracellular PAs on the rat muscle Na_V channel has disclosed only a small part of a complex phenomenon. Many important issues concerning this interaction remain to be addressed.

C.-J. H. is the recipient of a Brown-Coxe postdoctoral fellowship award from Yale Medical School. This work was supported by a grant from the National Institute of General Medical Sciences of the National Institutes of Health (GM-51172 to E. M).

REFERENCES

Amann, R., and E. Werle. 1956. On the complexes of heparin with histamine and other di- and polyamines. *Klinische Wochenschrift.* 34: 207–209.

Armstrong, C. M., and R. S. Croop. 1982. Simulation of Na channel inactivation by thiazin dyes. *J. Gen. Physiol.* 80:641–662.

Armstrong, C. M., and B. Hille. 1998. Voltage-gated ion channels and electrical excitability. *Neuron.* 20:371–380.

Bähring, R., D. Bowie, M. Benveniste, and M. L. Mayer. 1997. Permeation and block of GluR6 glutamate receptor channels by internal and external polyamines. *J. Physiol. (London).* 502.3:575–589.

Blaustein, R. O., and A. Finkelstein. 1990. Voltage-dependent block of anthrax toxin channels in planar bilayer membranes by symmetric tetraaklylammonium ions: effects on macroscopic conductance. *J. Gen. Physiol.* 96:905–919.

Cahalan, M. D., and W. Almers. 1979. Block of sodium conductance and gating current in squid giant axons poisoned with quaternary strychnine. *Biophys. J.* 27:57–74.

Catterall, W. A. 2000. From ionic currents to molecular mechanisms: the structure and function of voltage-gated sodium channels. *Neuron.* 26: 13–25.

Choi, K. L., R. W. Aldrich, and G. Yellen. 1991. Tetraethylammonium blockade distinguishes two inactivation mechanisms in voltage-activated K^+ channels. *Proc. Natl. Acad. Sci. USA.* 88:5092–5095.

Cullis, P. M., R. E. Green, L. Merson-Davies, and N. Travis. 1999. Probing the mechanisms of transport and compartmentalisation of polyamines in mammalian cells. *Chem. Biol.* 6:717–729.

Eaholz, G., A. Colvin, D. Leonard, C. Taylor, and W. A. Catterall. 1999. Block of brain sodium channels by peptide mimetics of the isoleucine, phenylalanine, and methionine (IFM) motif from the inactivation gate. *J. Gen. Physiol.* 113:279–293.

Favre, I., E. Moczydlowski, and L. Schild. 1996. On the structural basis for ionic selectivity among Na^+, K^+ and Ca^{2+} in the voltage-gated sodium channel. *Biophys. J.* 71:3110–3125.

Ficker, E., M. Taglialatela, B. A. Wible, C. M. Henley, and A. M. Brown. 1994. Spermine and spermidine as gating molecules for inward rectifier K^+ channels. *Science.* 266:1068–1072.

French, R. J., and J. B. Wells. 1977. Sodium ions as blocking agents and charge carriers in the potassium channel of the squid giant axon. *J. Gen. Physiol.* 70:707–724.

Garber, S. S. 1988. Symmetry and asymmetry of permeation through toxin-modified Na^+ channels. *Biophys. J.* 54:767–776.

Haghighi, A. P., and E. Cooper. 1998. Neuronal nicotinic acetylcholine receptors are blocked by intracellular spermine in a voltage-dependent manner. *J. Neurosci.* 18:4050–4062.

Haghighi, A. P., and E. Cooper. 2000. A molecular link between inward rectification and calcium permeability of neuronal nicotinic acetylcholine $\alpha3\beta4$ and $\alpha4\beta2$ receptors. *J. Neurosci.* 20:529–541.

Heinemann, S. H., H. Terlau, W. Stühmer, K. Imoto, K., and S. Numa. 1992. Calcium channel characteristics conferred on the sodium channel by single mutations. *Nature.* 356:441–443.

Hille, B. 1971. The permeability of the sodium channel to organic cations in myelinated nerve. *J. Gen. Physiol.* 58: 599–619.

Hille, B. 1992. Ionic Channels of Excitable Membranes, 2nd ed. Sinauer Associates, Sunderland, MA.

Huang, C.-J., I. Favre, and E. Moczydlowski. 2000. Permeation of large tetra-akylammonium cations through mutant and wild-type voltage-gated sodium channels as revealed by relief of block at high voltage. *J. Gen. Physiol.* 115:435–453.

Igarashi, K., and K. Kashiwagi. 2000. Polyamines: mysterious modulators of cellular functions. *Biochem. Biophys. Res. Comm.* 271:559–564.

Katz, B. 1949. Les constantes electriques de la membrane du muscle. *Archives de Science et Physiologie.* 2:285–299.

Lopatin, A. N., E. N. Makhina, and C. G. Nichols. 1994. Potassium channel block by cytoplasmic polyamines as the mechanism of intrinsic rectification. *Nature.* 372:366–369.

Lopatin, A. N., E. N. Makhina, and C. G. Nichols. 1995. The mechanism of inward rectification of potassium channels: "long-pore plugging" by cytoplasmic polyamines. *J. Gen. Physiol.* 106:923–955.

Lu, Z., and R. MacKinnon. 1994. Electrostatic tuning of Mg^{2+} affinity by an inward rectifier K^+ channel. *Nature* 371:243–246.

Lu, Z., and L. Ding. 1999. Blockade of a retinal cGMP-gated channel by polyamines. *J. Gen. Physiol.* 113:35–43.

Marty, A., and E. Neher. 1995. Tight-seal whole-cell recording. *In* Single-Channel Recording. B. Sakmann and E. Neher, eds. 2nd edition. Plenum Press, New York. 31–52.

Nichol, C. G., E. N. Makhina, W. L. Pearson, Q. Sha, and A. N. Lopatin. 1996. Inward rectification and implications for cardiac excitability. *Circ. Res.* 78:1–7.

Nichols, C. G., and A. N. Lopatin. 1997. Inward rectifier potassium channels. *Annu. Rev. Physiol.* 59:171–191.

O'Leary, M. E., R. G. Kallen, and R. Horn. 1994. Evidence for a direct interaction between internal tetra-alkylammonium cations and the inactivation gate of cardiac sodium channels. *J. Gen. Physiol.* 104:523–539.

O'Leary, M. E., and R. Horn. 1994. Internal block of human heart sodium channels by symmetrical tetra-alkylammoniums. *J. Gen. Physiol.* 104: 507–522.

Pusch, M. 1990. Open-channel block of Na^+ channels by intracellular Mg^{2+}. *Eur. Biophys. J.* 18:317–326.

Pusch, M., and E. Neher. 1988. Rates and diffusional exchange between small cell and a measuring patch pipette. *Pflügers Arch.* 411:204–211.

Ragsdale, D. S., J. C. McPhee, T. Scheuer, and W. A. Catterall. 1994. Molecular determinants of state-dependent block of Na^+ channels by local anesthetics. *Science.* 265:1724–1728.

Scheuer, T. 1999. A revised view of local anesthetic action: what channel state is really stabilized? *J. Gen. Physiol.* 113:3–6.

Scott, R. H., K. G. Sutton, and A. C. Dolphin. 1993. Interactions of polyamines with neuronal ion channels. *Trends Neurosci.* 16:153–160.

Sine, S. M., and J. H. Steinbach. 1984. Agonists block currents through acetylcholine receptor channels. *Biophys. J.* 46:277–284.

Sun, Y.-M., I. Favre, L. Schild, and E. Moczydlowski. 1997. On the structural basis for size-selective permeation of organic cations through the voltage-gated sodium channel: Effect of alanine mutations at the DEKA locus on selectivity, inhibition by Ca^{2+} and H^+, and molecular sieving. *J. Gen. Physiol.* 110:693–715.

Strichartz, G. R. 1973. The inhibition of sodium currents in myelinated nerve by quaternary derivatives of lidocaine. *J. Gen. Physiol.* 62:37–57.

Taglialatela, M., E. Ficker, B. A. Wible, and A. M. Brown. 1995. C-terminus determinants for Mg^{2+} and polyamine block of the inward rectifier K^+ channel IRK1. *EMBO J.* 14:5532–551.

Taylor, C. P., and L. S. Narasimhan. 1997. Sodium channels and therapy of central nervous system diseases. *Adv. Pharmacol.* 39:47–98.

Townsend, C., H. A. Hartmann, and R. Horn. 1997. Anomalous effect of permeant ion concentration on peak open probability of cardiac Na^+ channels. *J. Gen. Physiol.* 110:11–21.

Townsend, C., and R. Horn. 1999. Interaction between the pore and a fast gate of the cardiac sodium channel. *J. Gen. Physiol.* 113:321–331.

Trimmer, J. S., S. S. Cooperman, S. A. Tomiko, S. A. Zhou, S. M. Crean, M. B. Boyle, R. G. Kallen, Z. Sheng, R. L. Barchi, F. J. Sigworth, R. H. Goodman, W. S. Agnew, and G. Mandel. 1989. Primary structure and functional expression of a mammalian rat skeletal muscle sodium channel. *Neuron.* 3:33–49.

Williams, K. 1997. Interactions of polyamines with ion channels. *Biochem. J.* 325:289–297.

Woodhull, A. M. 1973. Ionic blockage of sodium channels in nerve. *J. Gen. Physiol.* 61:678–708.

Yang, J., P. T. Ellinor, W. A. Sather, J.-F. Zhang, and R. W. Tsien. 1993. Molecular determinants of Ca^{2+} selectivity and ion permeation in L-type Ca^{2+} channels. *Nature.* 366:158–161.

Yang, J., Y. N. Jan, and L. Y. Jan. 1995. Control of rectification and permeability in two distinct domains in an inward rectifier K^+ channel. *Neuron.* 14:1047–1054.

Yeh, J. Z., and T. Narahashi. 1977. Kinetic analysis of pancuronium interaction with sodium channels in squid axon membranes. *J. Gen. Physiol.* 69:293–323.